Cine-MRI Simulation to Evaluate Tumor Tracking

Tascón-Vidarte, José D.; Wahlstedt, Isak; Jomier, Julien; Erleben, Kenny; Vogelius, Ivan R.; Darkner, Sune

Published in:
Simulation and Synthesis in Medical Imaging - 6th International Workshop, SASHIMI 2021, Held in Conjunction with MICCAI 2021, Proceedings

Link to article, DOI:
10.1007/978-3-030-87592-3_13

Publication date:
2021

Document Version
Peer reviewed version

REAL-TIME DEFORMABLE REGISTRATION FOR TUMOR TRACKING DURING RADIOTHERAPY

José D. Tascón-Vidarte[1], *Isak Wahlstedt*[2,3], *Julien Jomier*[4],
Kenny Erleben[1], *Ivan R. Vogelius*[3], *Sune Darkner*[1]

[1]Department of Computer Science, University of Copenhagen, Copenhagen, Denmark
[2]Technical University of Denmark, Kongens Lyngby, Denmark
[3]Department of Oncology, Rigshospitalet, Copenhagen, Denmark
[4]Kitware SAS

ABSTRACT

We present a real-time tracking system based on a deformable registration algorithm for image-guided radiotherapy on a magnetic resonance (MR) linear accelerator. We evaluate the performance of five patients, receiving stereotactic body radiation therapy for liver metastases within a retrospective clinical study. Each patient had a pre-treatment 3D MR used as a reference and a 4DCT scan to capture breathing motion. The tumor and liver are delineated in the MR, and their positions at the video were estimated with registration. We tested the system with recorded 2D cine-MR videos acquired in the sagittal plane with 4 frames per second and evaluated the accuracy using 2D video simulations based on the respiratory motion. The video simulator generates ground truth segmentation of the tumor and the liver. Our method showed a Dice similarity coefficient between ground truth and registrations with mean values greater than 0.86 and 0.97 for tumor and liver respectively. The mean registration errors calculated with the tumor and the liver centers of mass were less than 0.9 and 0.4 mm respectively. The mean registration time per frame is 63 ms with a standard deviation of 42 ms on CPU allowing more than 4 frames per second. We demonstrate an accurate real-time tracking system for liver tumors.

Index Terms— Real-Time, Deformable Registration, Radiotherapy

1. INTRODUCTION

Current status and future challenges of magnetic resonance-guided (MR-guided) radiotherapy are exposed in [1]. Among the current trend of in-room MR radiotherapy systems, there is one noticeable device called a magnetic resonance linear accelerator (MR-linac), defined as a magnetic resonance scanner combined with a linear accelerator. In radiotherapy, the term beam gating is used whenever the treatment accelerator beam is triggered in response to patient movement [2], e.g breathing motion. MR-linacs with the capability of intra-treatment 2D visualization and gating of internal anatomy has recently become commercially available with the MRIdian system (ViewRay Inc., USA) [3] and with the Elekta-Unity system [4].

Stereotactic body radiotherapy (SBRT) of liver metastases on such a system is advantageous both due to improved soft-tissue contrast compared to cone-beam computed tomography and due to the ability for internal gating [5]. Clinical advantages of liver SBRT using an MR-linac with online tracking have been demonstrated in [6], where the potential benefit is to reduce the liver target volume up to 30% and therefore a lower radiation dose to the adjacent normal tissue and organs.

Liver tumors deform and move during treatment mainly caused by breathing motion [7]. During treatment, the scanner acquires 2D cine-MR sagittal images at 4 frames per second. A main component of the MR-Linac system to achieve beam gating is the tumor tracking. The tumor tracking problem is solved automatically using image analysis. Some proposed strategies for tumor tracking are based on template matching [8], feature detection [9], optical-flow methods [10, 11], segmentation [12] neuronal networks [13] or modeling based [14]. Fast et al. [15] presented a comparative study where they analyze the feasibility of most of the mentioned tracking techniques. The authors conclude that the different algorithms all have relatively similar performance.

One of the issues that we perceive is that the current tracking systems may fail to unexpected movements due to their design, i.e. to have a subset of images (templates) to compare intensity similarity and then estimate position. Some of these tracking flaws have been noticed during treatment at our institution. Furthermore, current systems are only capable of tracking single objects. That is why we exhibit here a general tracking system based on deformable registration, that can capture the full motion geometry during treatment without any prior motion knowledge or pre-recorded templates. To the best of our knowledge, this is the first real-time deformable registration that can process the cine-MR frame rate. Our code is available at https://github.com/josetascon/imart/.

2. METHODS

2.1. Data

This study uses image data from five patients already treated with SBRT for metastases in the liver at Rigshospitalet (Copenhagen, Denmark) between April and December 2019. The patients provided consent and approval for the usage of their anonymized data for research purposes.

Respiratory correlated 4DCT with intravenous contrast injection was performed for all patients on a SOMATOM Definition AS scanner (Siemens Healthineers, Germany). 4DCT image data were phase-sorted into ten phase bins throughout a respiratory cycle based on an external respiratory signal monitored with Real-Time Position Management (RPM, Varian Medical Systems, Palo Alto, CA). The slice separation in each phase of the 4DCT was 2 mm. The image resolution in each slice was 512×512 pixels and a pixel size of 0.98×0.98 mm.

Additionally, MR scans in inspiration breath-hold without visual guidance were performed for all patients. The 3D MR images were acquired in a 0.3T MRIDIAN MR-Linac (ViewRay, USA). The acquisition technique is balanced steady-state free precession (bSSFP). The pre-treatment image is in 3D with a resolution of [$512 \times 512 \times 128$ pixels] and [$1.5 \times 1.5 \times 3.0$ mm] spacing. The video images are 2D cine-MR (bSSFP-Sagittal) with a resolution of [512×512 pixels] and [1.5×1.5 mm] spacing.

The clinical Gross Tumor Volume (GTV) was delineated on the 3D MR by a senior radiologist and approved by a senior oncologist. Risk organs, including the liver, were also delineated. These delineations are used to segment the region of interest (ROI).

2.2. Tracking System

We propose a tracking system based on real-time deformable registration. The system is depicted in Figure 1. A 2D slice is extracted from a 3D treatment MR image as a fixed reference for registration. The slice is manually selected during treatment based on where the tumor is best visualized. Each input cine-MR image from the time series during treatment is registered to the reference and the GTV ROI is used to locate the tumor. This study aims to achieve a deformable registration within 250 ms (4 frames per second).

2.3. Algorithm

We chose to implement the diffeomorphic demons as a fast solution [16]. The computational bottleneck of registration is the computation of the transformation and the similarity metric [17]. We primary focus on this stage to improve performance. Our registration algorithm is implemented on C++ and parallelized on CPU with OpenMP.

Having $\varphi(x)$ as the diffeomorphic transformation field (referred as φ_x for simplicity), I_0 as the fixed image and I_1 as the moving image, the demons algorithm defines the deformation field update as:

$$F(\nabla E(\varphi_x)) \equiv \frac{(I_0 - I_1(\varphi_x))\nabla I_1(\varphi_x)}{\|\nabla I_1(\varphi_x)\|^2 + (I_0 - I_1(\varphi_x))^2} \quad (1)$$

The iterative process to update the transformation $\varphi(x)$ is defined as:

$$\begin{aligned} compute: &\quad u(x) = F(\nabla E(\varphi(x))) \\ fluid\,update: &\quad u(x) \leftarrow G^{\sigma_f} * u(x) \\ diffeomorphic: &\quad \varphi(x)' \leftarrow exp(u(x)) \\ diffusion\,update: &\quad \varphi(x) \leftarrow G^{\sigma_d} * \varphi(x)' \end{aligned} \quad (2)$$

Where G refers to a gaussian kernel. The expression $exp()$ refers to the intrinsic update on the Lie group of diffeomorphisms. For more details please refer to Vercauten et al. [16].

2.4. Video Simulation

We develop a video simulator to generate ground truth data to evaluate the registration algorithm accuracy. We use the 4DCT scan that represents the full respiratory cycle of each patient. Initially, all phases in the 4DCT are registered sequentially with the symmetric normalization algorithm [18]. Afterward, the MR image is registered to phase 00 of the 4DCT scan, since both images are at inspiration position. This transformed MR is the starting video image. The simulator produces each new video frame with a composition of sequential transformations related to the 4DCT. The corresponding transformation is interpolated over time to match the proportion of the respiratory cycle with the video sample time. For each patient, we generate 20 seconds of a video, approximately 4-5 breathing cycles of the patient. The resulting videos are visually close to the cine-MR.

Since the initial delineations of the tumor and liver are known in the reference MR, we create independent files with those regions of interest (ROI). The ROI files are also transformed in parallel to the raw video image generation. Therefore, we have the ground truth ROI for each video sample. This approach is equivalent to have the radiologist delineation (segmentation) at each frame.

The video is created based on 3D images and transformations and then, a 2D slice is extracted in the sagittal view where the tumor has wider visibility. Therefore the simulation video contains the complexity of real 3D motion in the 2D images. This process resembles the MR-Linac treatment setup, where 2D real-time images are tracked.

2.5. Metrics

We collect statistical results for the whole video of each patient. Each input image is registered to the reference and com-

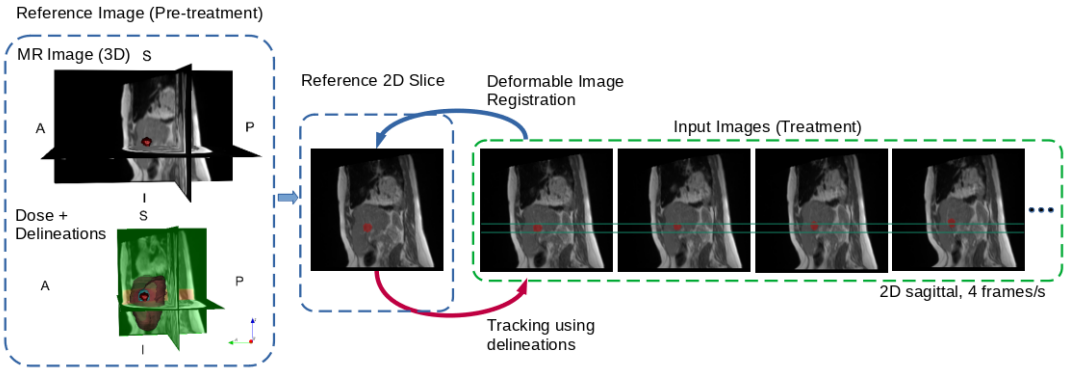

Fig. 1. Proposed pipeline of a real-time deformable registration algorithm used for tumor tracking in liver radiotherapy.

pared to the ground truth value. We use two metrics to check the tracking capabilities of the algorithm.

The first metric used is Dice Similarity Coefficient (DSC). The dice metric is defined as follows:

$$DSC(X,Y) \equiv \frac{2|X \cap Y|}{|X| + |Y|} \tag{3}$$

In our case, DSC evaluates area correspondence in the ROI. The video sequences contain as ROIs the gross tumor volume (GTV) and liver at each frame. The DSC metric is calculated between the ground truth and the registered ROI. The registered ROI is found by transforming the reference to the current input image. This transformation is estimated in real-time. Statistical results are collected offline.

The second metric is the registration error computed for the center of mass. The registration error is calculated as the euclidean distance between the ground truth position of the landmark and the estimated position of the landmark. The ground truth coordinate is a point x_t, where the subscripts t refer to time, i.e. a particular image in the video. The transformation found by registration φ_t was applied to the landmark reference position x_{init}, producing the estimated landmark $\hat{x}_t = \varphi_t \circ x_{\text{init}}$. The registration error is defined as:

$$r_{\text{error}} \equiv \|x_t - \varphi_t \circ x_{\text{ref}}\| \tag{4}$$

The center of mass of GTV and liver are compared between the transformed and ground truth in the video. We follow the same procedure as before to collect the statistical results.

To validate that the registration algorithm is working, we compare each metric with the baseline. In particular, the baseline for the DSC and the registration error is calculated comparing the reference image against each input image without registration. This will produce at maximum breathing displacement a DSC closer to zero and larger values of distance error. The statistical results of a full video should reflect also a wider distribution for the baseline compared to the registered ROIs.

Patient	1	2	3	4	5
Tumor location (geometric)	S-A-L	S-A-L	S-A-R	S-P-L	I-P-R
Breathing cycle (mean) [s]	4.8	3,0	4.1	4.1	5.8
Tumor max. displacement [mm]	3.9	9.8	8.1	6.5	12.6
Tumor volume [cm3]	5.5	5.6	12.0	8.0	5.7
Tumor sagittal area [cm2]	2.7	3.0	7.4	4.7	4.1
Liver volume [cm3]	1979	1782	1876	1411	895
Liver sagittal area [cm2]	120.2	131.4	109.7	94.0	90.8
Registration mean time [ms]	44.3	37.5	59.2	68.5	105.7
Registration std. dev. time [ms]	12.8	11.2	29.9	25.1	42.7

Table 1. Summary of patient information. Tumor location is the geometric octant of where the tumor is with regards to the liver COM. The abbreviations correspond to Superior-Inferior, Anterior-Posterior, and Left-Right. Breathing cycle times were determined from real patient respiratory motion during 4DCT scans. Tumor displacements refer to the maximum motion presented in the video without registration. GTV and liver volumes/areas are estimated on the reference 3D/2D (sagittal) MR. Registration times for each patient video are estimated with mean and standard deviation. COM = center of mass.

3. RESULTS

All the tests are run on a workstation with 2 CPUs and 128 GB of RAM. Each CPU is an Intel(R) Xeon(R) Silver 4110 @ 2.10GHz, 8 cores, 16 threads. We benchmark transformations-interpolations and registration and found better behavior when using 8 threads. All the tests reported below were run using 8 threads (a single CPU).

Table 1 summarize the patient conditions of tumor and breathing motion. We also show here the registration times with mean values and standard deviation. The patient set is small in number but represent a wide variety of breathing and tumor motion conditions.

We test the system with the real MR-Linac recorded images and prove that registration is working within the restricted time. The overall registration time is computed with mean values 62.7 ms and a standard deviation of 42.3 ms. The maximum registration time is 242 ms, this value is obtained

for one image of patient 5 where maximum displacement is given. Furthermore, visual registration quality is obtained. However, the videos from our simulation are used to properly test the system in terms of accuracy.

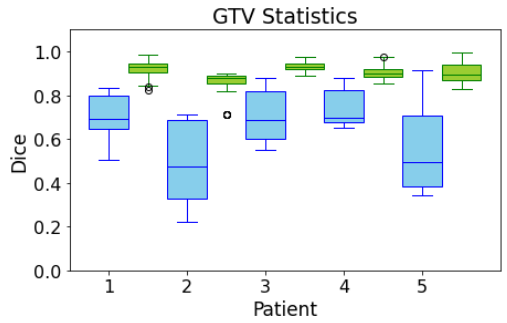

(a) Gross tumor volume.

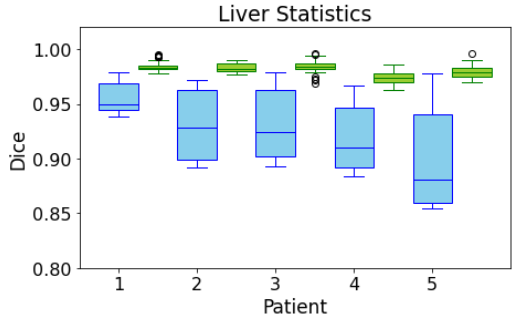

(b) Liver.

Fig. 2. Video statistics of dice similarity coefficient. The metric is estimated for each patient with all the input images of simulated video. In blue, the baseline as the metric computed without registration. Adjacent in green, the dice values determined with registration.

The video statistics of the Dice similarity coefficient are visualized in Figure 3. Figure 3 (a) relates to GTV and (b) to liver. The baseline is shown in blue for each patient and next to it the registration values in green. The GTV baseline that corresponds to the metric without registration shows less overlapping areas during the respiratory movement for patient 4 and a major overlapping area for patient 2 during the video. The registration produces statistically different behavior in the dice metric, i.e. indication of proper behavior. The best cases are for patient 3 and 4 with dice $mean \pm std.dev.$ of 0.93 ± 0.02 and 0.9 ± 0.03 respectively. Those could be explained because patient 3 has a larger visible area of the tumor and patient 4 due to major overlapping areas, both conditions facilitate the registration task. The worst case is for patient 2 with dice values of 0.86 ± 0.05. The metric computed for liver offer better registration results due to the larger area within the sagittal image, worst-case patient 4 with $mean \pm std.dev.$ 0.97 ± 0.006.

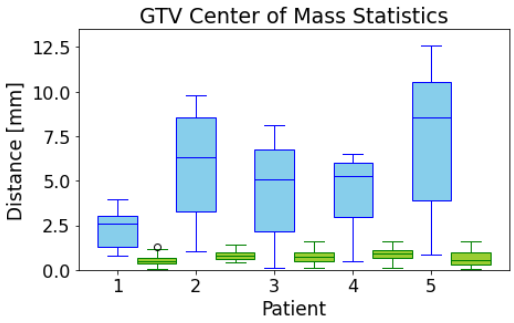

(a) Gross tumor volume.

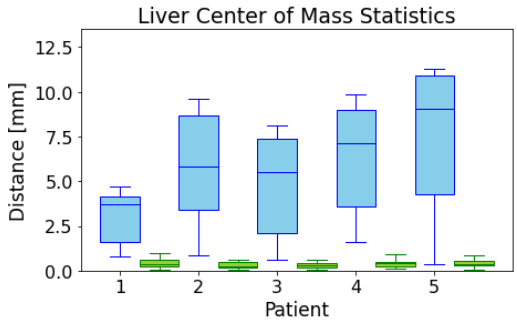

(b) Liver.

Fig. 3. Video statistics of registration errors using the center of mass. The metric is computed for each patient with all the input images of simulated video. In blue, the baseline as the motion distance without registration. Adjacent in green, the distance errors determined with registration.

Figure 3 shows the video statistics of the registration error of the center of mass. Figure 3 (a) relates to GTV and (b) to liver. Again, we display in blue the baseline and in green with registration. This metric baseline reflects the respiratory motion which is less for patient 1 and greater patient 5. Registration produces good results with distances lower than 1.6 mm in the worst case. This value is adequate and tolerable considering image spacing of 1.5 mm. The worst-case registration is patient 2 with values 0.9 ± 0.3 mm. The results of this metric are a significant indicator that the tracking is successful even for patients with wider respiratory motion.

4. CONCLUSION

We demonstrate the implementation of a successful real-time tracking system based on a deformable registration algorithm that is suitable for image-guided radiotherapy on MR-Linac. We prove the system with the respiratory motion of five (5) patients. The registration time has a mean value of 62 ms and a maximum value of 247 ms. As opposed to the existing tracking system, our system could be capable of tracking multiple organs, due to the full registration.

5. COMPLIANCE WITH ETHICAL STANDARDS

This is a retrospective study without biological data and patients signed informed consent for use of the medical image data for research. A subset of 2 of the patients (patient 4 and 5) were selected from an ethical committee approved study (approval nr. H-17033786) that investigates liver SBRT in breath-hold. The remainder patients were treated according to standard practice in the department, in line with the principles of the Declaration of Helsinki.

6. ACKNOWLEDGMENTS

We would like to acknowledge Signe Risum (MD) and Kristian Boye for their support related to patient treatment and technical assistance with MR-Linac.

This project has received funding from the European Union's Horizon 2020 research and innovation program under the Marie Sklodowska-Curie grant agreement No. 764644. This paper only contains the author's views and the Research Executive Agency and the Commission are not responsible for any use that may be made of the information it contains.

7. REFERENCES

[1] Chiara Paganelli, B Whelan, Marta Peroni, Paul Summers, M Fast, Tessa van de Lindt, J McClelland, Björn Eiben, P Keall, T Lomax, et al., "Mri-guidance for motion management in external beam radiotherapy: current status and future challenges," *Physics in Medicine & Biology*, vol. 63, no. 22, pp. 22TR03, 2018.

[2] SPM Crijns, JGM Kok, JJW Lagendijk, and BW Raaymakers, "Towards mri-guided linear accelerator control: gating on an mri accelerator," *Physics in Medicine & Biology*, vol. 56, no. 15, pp. 4815, 2011.

[3] Jeffrey Olsen, Olga Green, and Rojano Kashani, "World's first applicaton of mr-guidance for radiotherapy," *Missouri medicine*, vol. 112, no. 5, pp. 358, 2015.

[4] BW Raaymakers, IM Jürgenliemk-Schulz, GH Bol, M Glitzner, ANTJ Kotte, B Van Asselen, JCJ De Boer, JJ Bluemink, SL Hackett, MA Moerland, et al., "First patients treated with a 1.5 t mri-linac: clinical proof of concept of a high-precision, high-field mri guided radiotherapy treatment," *Physics in Medicine & Biology*, vol. 62, no. 23, pp. L41, 2017.

[5] C Kontaxis, GH Bol, B Stemkens, M Glitzner, FM Prins, LGW Kerkmeijer, JJW Lagendijk, and BW Raaymakers, "Towards fast online intrafraction replanning for free-breathing stereotactic body radiation therapy with the mr-linac," *Physics in Medicine & Biology*, vol. 62, no. 18, pp. 7233, 2017.

[6] Shahad Al-Ward, Matt Wronski, Syed Bilal Ahmad, Sten Myrehaug, William Chu, Arjun Sahgal, and Brian M Keller, "The radiobiological impact of motion tracking of liver, pancreas and kidney sbrt tumors in a mr-linac," *Physics in Medicine & Biology*, vol. 63, no. 21, pp. 215022, 2018.

[7] Martin J Murphy, "Tracking moving organs in real time," in *Seminars in radiation oncology*. Elsevier, 2004, vol. 14, pp. 91–100.

[8] Lau Brix, Steffen Ringgaard, Thomas Sangild Sørensen, and Per Rugaard Poulsen, "Three-dimensional liver motion tracking using real-time two-dimensional mri," *Medical physics*, vol. 41, no. 4, pp. 042302, 2014.

[9] Chiara Paganelli, Matteo Seregni, Giovanni Fattori, Paul Summers, Massimo Bellomi, Guido Baroni, and Marco Riboldi, "Magnetic resonance imaging–guided versus surrogate-based motion tracking in liver radiation therapy: a prospective comparative study," *International Journal of Radiation Oncology* Biology* Physics*, vol. 91, no. 4, pp. 840–848, 2015.

[10] Cornel Zachiu, Nicolas Papadakis, Mario Ries, Chrit Moonen, and B Denis De Senneville, "An improved optical flow tracking technique for real-time mr-guided beam therapies in moving organs," *Physics in Medicine & Biology*, vol. 60, no. 23, pp. 9003, 2015.

[11] Matteo Seregni, Chiara Paganelli, Paul Summers, Massimo Bellomi, Guido Baroni, and Marco Riboldi, "A hybrid image registration and matching framework for real-time motion tracking in mri-guided radiotherapy," *IEEE Transactions on Biomedical Engineering*, vol. 65, no. 1, pp. 131–139, 2017.

[12] S Gou, J Wu, F Liu, P Lee, S Rapacchi, P Hu, and K Sheng, "Feasibility of automated pancreas segmentation based on dynamic mri," *The British journal of radiology*, vol. 87, no. 1044, pp. 20140248, 2014.

[13] Jihyun Yun, Eugene Yip, Zsolt Gabos, Keith Wachowicz, Satyapal Rathee, and BG Fallone, "Neural-network based autocontouring algorithm for intrafractional lung-tumor tracking using linac-mr," *Medical physics*, vol. 42, no. 5, pp. 2296–2310, 2015.

[14] Noemi Garau, Riccardo Via, Giorgia Meschini, Danny Lee, Paul Keall, Marco Riboldi, Guido Baroni, and Chiara Paganelli, "A roi-based global motion model established on 4dct and 2d cine-mri data for mri-guidance in radiation therapy," *Physics in Medicine & Biology*, vol. 64, no. 4, pp. 045002, 2019.

[15] Martin F Fast, Björn Eiben, Martin J Menten, Andreas Wetscherek, David J Hawkes, Jamie R McClelland, and Uwe Oelfke, "Tumour auto-contouring on 2d cine mri for locally advanced lung cancer: A comparative study," *Radiotherapy and Oncology*, vol. 125, no. 3, pp. 485–491, 2017.

[16] Tom Vercauteren, Xavier Pennec, Aymeric Perchant, and Nicholas Ayache, "Diffeomorphic demons: Efficient non-parametric image registration," *NeuroImage*, vol. 45, no. 1, pp. S61–S72, 2009.

[17] Ramtin Shams, Parastoo Sadeghi, Rodney A Kennedy, and Richard I Hartley, "A survey of medical image registration on multicore and the gpu," *IEEE signal processing magazine*, vol. 27, no. 2, pp. 50–60, 2010.

[18] Brian B Avants, Charles L Epstein, Murray Grossman, and James C Gee, "Symmetric diffeomorphic image registration with cross-correlation: evaluating automated labeling of elderly and neurodegenerative brain," *Medical image analysis*, vol. 12, no. 1, pp. 26–41, 2008.